

# Functional Synthetic Model for the Lanthanide-Dependent Quinoid Alcohol Dehydrogenase Active Site

Alex McSkimming, Thibault Cheisson,<sup>ID</sup> Patrick J. Carroll, and Eric J. Schelter<sup>\*ID</sup>

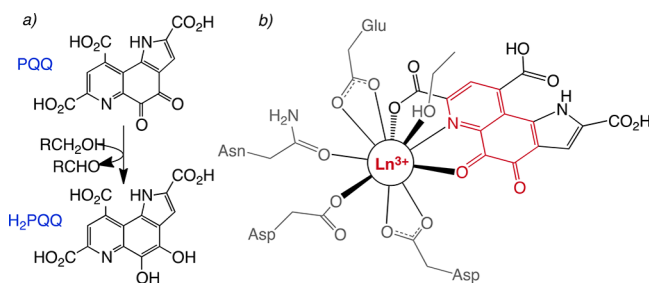
P. Roy and Diana T. Vagelos Laboratories, Department of Chemistry, University of Pennsylvania, 231 S 34th Street, Philadelphia, Pennsylvania 19104, United States

## Supporting Information

**ABSTRACT:** The oxidation of methanol by dehydrogenase enzymes is an essential part of the bacterial methane metabolism cycle. The recent discovery of a lanthanide (Ln) cation in the active site of the XoxF dehydrogenase represents the only example of a rare-earth element in a physiological role. Herein, we report the first synthetic, functional model of Ln-dependent dehydrogenase and its stoichiometric and catalytic dehydrogenation of a benzyl alcohol. Density functional theory calculations implicate a hydride transfer mechanism for these reactions.

Methanol dehydrogenase (MDH) enzymes play an important role in the global carbon cycle, namely through the bacterial methane metabolism pathway, by catalyzing the oxidation of methanol.<sup>1</sup> The active site of MDH enzymes contains a pyrroloquinoline quinone (PQQ) cofactor bound to a  $\text{Ca}^{2+}$  ion, which accepts formally two electrons and two protons from an alcohol substrate to afford the corresponding aldehyde and catechol ( $\text{H}_2\text{PQQ}$ , Scheme 1a).<sup>2</sup> It was recently demonstrated that early lanthanide ions:

**Scheme 1.** (a) Reaction between Cofactor PQQ and Alcohol Substrates To Give Catechol  $\text{H}_2\text{PQQ}$  and (b) Active Site of Ln-Dependent MDH from XRD Data with Bound EtOH Ligand



La–Nd accelerated alcohol metabolism, and in one case were essential for cell growth of certain methanotrophic bacteria.<sup>3</sup> An X-ray structure of the XoxF-type MDH enzyme from *Methylophilum fumariolicum* SoIV revealed a  $\text{Ln}^{3+}$  cation bound by the PQQ cofactor (Scheme 1b),<sup>3d</sup> the first example of a lanthanide (or rare-earth) element in a physiological role. Lanthanides evidently confer a competitive advantage over  $\text{Ca}^{2+}$ , with XoxF-MDH displaying a 10-fold higher methanol affinity constant than Ca-MDHs.<sup>3d,4</sup> Furthermore, Ca-MDHs

exhibit highest activities at  $\text{pH} \sim 9$  whereas XoxF-MDH functions optimally at neutral pH and does not require ammonium ions for activation.<sup>3d,4</sup> Also, in contrast to Ca-MDHs, XoxF-MDH catalyzes the oxidation of formaldehyde to formate.<sup>3d,4</sup>

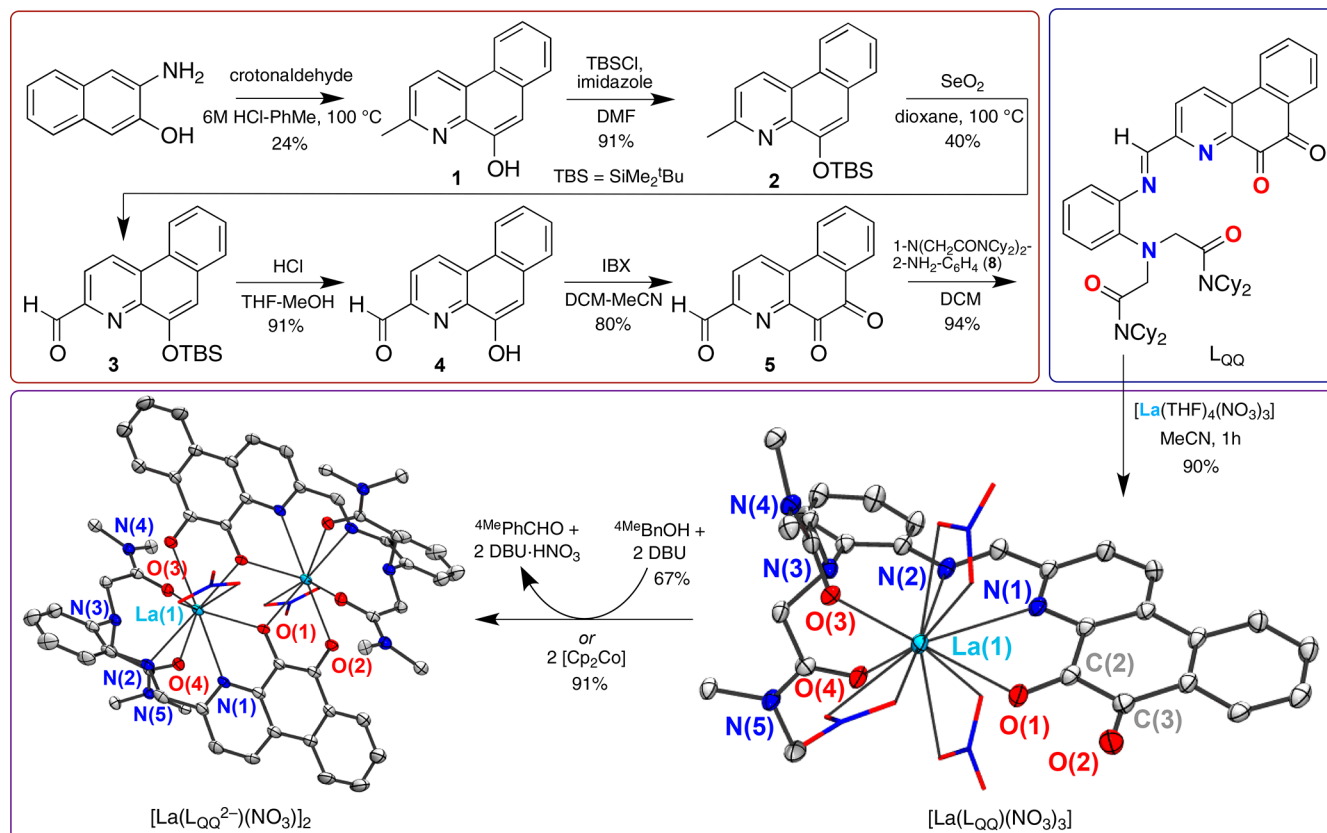
The study of well-defined synthetic model compounds is essential for understanding the workings of enzyme active sites, which in turn may inspire novel catalysts.<sup>5</sup> At present, however, reports of synthetic metal complexes of PQQ or analogues are scarce<sup>6</sup> and only a handful of such compounds have been structurally characterized.<sup>7</sup> Furthermore, their reactivity has typically not been reported, with a few exceptions.<sup>6a–e</sup> To date, there are no reports of a synthetic lanthanide complex of PQQ or its surrogates.

There are a number of challenges associated with synthesizing analogues of MDH active sites. First, PQQ derivatives may coordinate to a metal ion in non-natural binding modes, such as through the two quinone oxygen atoms<sup>7c,d</sup> or the distal pyrrole and carboxylic acid groups.<sup>7a</sup> Multiple quinoline quinones (QQs) may also bind a single metal center or otherwise exhibit complicated speciation.<sup>8</sup> To overcome these potential problems, we designed the ligand  $\text{L}_{\text{QQ}}$  (Scheme 2), which incorporated a directing and sterically bulky chelator. An important goal of this design was the structural characterization of metal complexes of  $\text{L}_{\text{QQ}}$  and the product(s) of their reaction with substrates. We report herein the synthesis of  $\text{L}_{\text{QQ}}$ , its corresponding lanthanum complex  $[\text{La}(\text{L}_{\text{QQ}})(\text{NO}_3)_3]$  and its stoichiometric and catalytic dehydrogenation of a benzyl alcohol substrate.

Proligand  $\text{L}_{\text{QQ}}$  was synthesized in 11 steps from commercially available starting materials (Scheme 2). Metalation of  $\text{L}_{\text{QQ}}$  proceeded smoothly using  $[\text{La}(\text{NO}_3)_3(\text{THF})_4]$  to obtain  $[\text{La}(\text{L}_{\text{QQ}})(\text{NO}_3)_3]$  in 90% yield as a moisture-sensitive orange solid (Scheme 2).  $[\text{La}(\text{L}_{\text{QQ}})(\text{NO}_3)_3]$  is a rare example of a metal complex of a quinoline quinone<sup>7</sup> and is the first such lanthanide complex. The X-ray crystal structure of  $[\text{La}(\text{L}_{\text{QQ}})(\text{NO}_3)_3]$  revealed La(1) to bound to the pyridyl nitrogen atom N(1) and a single quinone oxygen O(1) of the QQ moiety (Scheme 2 and S1), analogous to the coordination environment of the XoxF enzyme active site (Scheme 1).<sup>3d,4</sup> Cyclic voltammograms (CVs) performed on  $\text{L}_{\text{QQ}}$  revealed a largely reversible process at  $E_{1/2} = -0.95 \text{ V}$  vs  $\text{Fc}/\text{Fc}^+$  for the quinone–semiquinone ( $\text{QQ}/\text{QQ}^{\bullet-}$ ) couple (Figure 1, dashed line) followed by an irreversible process at  $E_c = -1.76 \text{ V}$

Received: November 21, 2017

Published: December 29, 2017

Scheme 2. Synthesis of  $\text{L}_{\text{QQ}}$  [ $\text{La}(\text{L}_{\text{QQ}})(\text{NO}_3)_3$ ] and [ $\text{La}(\text{L}_{\text{QQ}}^{2-})(\text{NO}_3)_3$ ] $_2$  with 50% Thermal Ellipsoid Plots<sup>a</sup>

<sup>a</sup>H-atoms have been omitted, cyclohexyl groups have been truncated and  $\text{NO}_3^-$  ligands are displayed in wireframe for clarity.

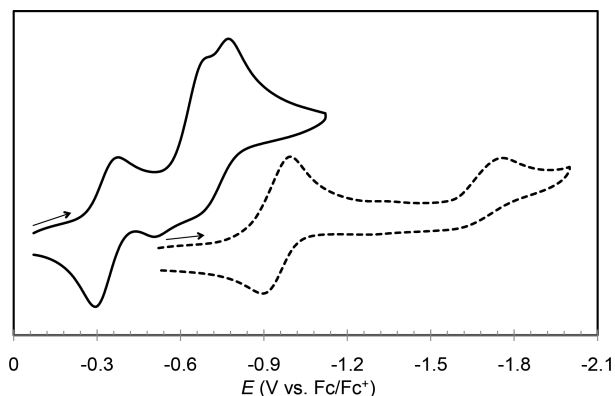


**Figure 1.** Cyclic voltammograms of  $[\text{La}(\text{L}_{\text{QQ}})(\text{NO}_3)_3]$  (solid line) and  $\text{L}_{\text{QQ}}$  (dashed line) in  $\text{CH}_2\text{Cl}_2$  with 0.1 M  $[\text{nPr}_4\text{N}][\text{BARF}_4]$  at a scan rate of 100  $\text{mV s}^{-1}$ .

assigned as formation of the catechololate dianion ( $\text{Q}^{2-}$ ).<sup>9</sup> For  $[\text{La}(\text{L}_{\text{QQ}})(\text{NO}_3)_3]$ , the  $\text{QQ}/\text{QQ}^{2-}$  couple was observed at +0.61 V higher potential ( $E_{1/2} = -0.34$  V;  $i_a/i_c \approx 0.8$  at 100  $\text{mV s}^{-1}$ , Figure 1, solid line.) Two poorly reversible, overlapping reduction events were revealed on further cathodic sweeps at  $-0.68$  and  $-0.77$  V, which showed return waves at  $-0.66$  and  $-0.52$  V. Overall, the CV of  $[\text{La}(\text{L}_{\text{QQ}})(\text{NO}_3)_3]$  was complicated by loss of  $\text{NO}_3^-$  ligand(s) and dimerization equilibria (*vide infra*); the waves were not definitively assigned (Figures S31–36). Importantly, the anodic shift of the  $\text{QQ}/\text{QQ}^{2-}$  couple for  $[\text{La}(\text{L}_{\text{QQ}})(\text{NO}_3)_3]$  compared to  $\text{L}_{\text{QQ}}$  reflected stabilization of the  $\text{QQ}^{2-}$  anion by the bound metal ion.<sup>9a,10</sup>

We expected that the relative ease of reduction of the QQ moiety upon coordination to La would be reflected in the ability of  $[\text{La}(\text{L}_{\text{QQ}})(\text{NO}_3)_3]$  to oxidize an alcohol substrate. A  $\text{CD}_2\text{Cl}_2$  solution of free ligand  $\text{L}_{\text{QQ}}$  with a 4-fold excess of  $4\text{MeBnOH}$ <sup>11</sup> gave no detectable aldehyde product by  $^1\text{H}$  NMR spectroscopy, upon mixing, even after 3 days. In contrast,  $[\text{La}(\text{L}_{\text{QQ}})(\text{NO}_3)_3]$  reacted with 2.5 equiv  $4\text{MeBnOH}$  in  $\text{CD}_2\text{Cl}_2$  to produce  $4\text{MePhCHO}$  in 30% yield in 24 h (67% yield in 3 days, Table S3). As observed by Itoh and Fukuzumi in a related system,<sup>6b,c</sup> addition of 2.2 equiv DBU accelerated the dehydrogenation of  $4\text{MeBnOH}$  by  $[\text{La}(\text{L}_{\text{QQ}})(\text{NO}_3)_3]$  with  $4\text{MePhCHO}$  produced in  $63 \pm 3\%$  yield ( $^1\text{H}$  NMR spectroscopy) in  $<10$  min with completion of the reaction at this point. No detectable quantity of  $4\text{MePhCO}_2\text{H}$  was produced and only broad, indistinct peaks for  $\text{L}_{\text{QQ}}$  containing product(s) were observed (Figure S29). Performing the reaction on a preparative scale gave pure, black-green  $[\text{La}(\text{L}_{\text{QQ}}^{2-})(\text{NO}_3)_3]_2$  in 67% yield. This dimer was also synthesized from  $[\text{La}(\text{L}_{\text{QQ}})(\text{NO}_3)_3]$  and 2 equiv  $[\text{Cp}_2\text{Co}]$  (91%; Scheme 2). The considerably less basic, and thus more physiologically relevant, 2,6-lutidine could be substituted for DBU ( $\text{pK}_a \sim 7$  cf.  $\sim 12$  for DBU).<sup>12</sup> The reaction, while slower, was still much faster (complete in  $<24$  h) than that in the absence of a base, and gave  $4\text{MePhCHO}$  in 37% yield (Table S3). A control reaction of  $\text{L}_{\text{QQ}}$  with 1.2 equiv  $4\text{MeBnOH}$  and 2.2 equiv DBU produced only trace amounts ( $<3\%$  yield) of  $4\text{MePhCHO}$  in 30 min (13% after 4 h).  $[\text{La}(\text{L}_{\text{QQ}}^{2-})(\text{NO}_3)_3]_2$  is the first structurally characterized metal complex of a reduced quinoline quinone. Notably, Itoh and Fukuzumi assigned the product of the reaction of  $\text{PQQ}$ -trimethylester ( $\text{PQQTME}$ ),  $\text{Ca}^{2+}$ , an alcohol and DBU as a

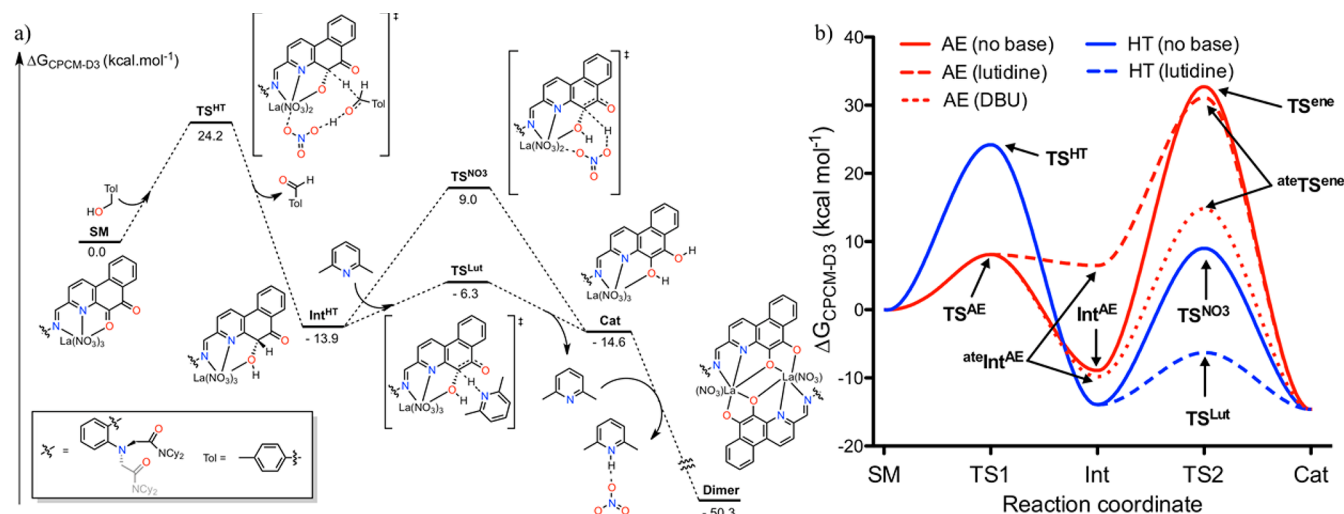


**Figure 2.** DFT-calculated reaction coordinates for the dehydrogenation of  $4^{\text{Me}}\text{BnOH}$  by  $[\text{La}(\text{LQQ})(\text{NO}_3)_3]$ : (a) a 2,6-lutidine-assisted HT mechanism; (b) comparison of the AE (red traces) and HT (blue traces) mechanisms in the absence of base (solid traces) and the influence of DBU (dotted trace) or 2,6-lutidine (dashed traces).

monomeric, singly deprotonated catechol complex,<sup>6b</sup> in contrast to fully deprotonated  $[\text{La}(\text{LQQ}^{2-})(\text{NO}_3)_3]$ .

We hypothesized that, with a suitable terminal oxidant and base, the dehydrogenation of  $4^{\text{Me}}\text{BnOH}$  by  $[\text{La}(\text{LQQ})(\text{NO}_3)_3]$  could be performed catalytically. A mixture of 1 equiv  $4^{\text{Me}}\text{BnOH}$ , 2 equiv  $[\text{Fc}][\text{PF}_6]$ , 2 equiv 2,6-lutidine (as DBU was incompatible with  $[\text{Fc}]^+$  salts) and  $[\text{La}(\text{LQQ})(\text{NO}_3)_3]$  (5 mol %) in  $\text{CD}_2\text{Cl}_2$ – $\text{CD}_3\text{CN}$  (2:1 v/v) was monitored by  $^1\text{H}$  NMR spectroscopy (Figure S30). In <20 min, characteristic peaks corresponding to  $4^{\text{Me}}\text{PhCHO}$  were observed. After 21 h,  $4^{\text{Me}}\text{PhCHO}$  had been produced in 84% yield (~17 turnovers) with 85% of the  $4^{\text{Me}}\text{BnOH}$  having been consumed, indicating clean conversion. Extending the reaction another 24 h increased the yield of aldehyde to 96%. In the absence of  $[\text{La}(\text{LQQ})(\text{NO}_3)_3]$ , no  $4^{\text{Me}}\text{PhCHO}$  was produced within 24 h under these conditions. Replacing  $[\text{La}(\text{LQQ})(\text{NO}_3)_3]$  with 5 mol %  $[\text{La}(\text{THF})_4(\text{NO}_3)_3]$  or  $\text{LQQ}$  gave  $4^{\text{Me}}\text{PhCHO}$  in 5% or 14% yield, respectively, after 21 h. These results show the requirements of both La and the LQQ ligand for catalytic turnover. The dehydrogenation of ~60 mg of  $4^{\text{Me}}\text{BnOH}$ , catalyzed by  $[\text{La}(\text{LQQ})(\text{NO}_3)_3]$ , was carried out under the above conditions to afford  $4^{\text{Me}}\text{PhCHO}$  and Fc in 75% and 83% isolated yields, respectively, in 24 h. Itoh and Fukuzumi reported dehydrogenation of ethanol (~15 turnovers in 65 h) by a mixture of  $[\text{Ca}(\text{ClO}_4)_2]$ , PQQTME, DBU and  $\text{O}_2$ .<sup>6b</sup> Until our report, theirs was the only nonbiological example of alcohol dehydrogenation catalyzed by a metal complex of a PQQ derivative. Notably, our system does not employ  $\text{O}_2$ , which may oxidize the aldehyde to give carboxylic acid byproducts.

For further insights into the reactivity and properties of  $[\text{La}(\text{LQQ})(\text{NO}_3)_3]$ , we turned to computations. The gas-phase structures of  $\text{LQQ}$ ,  $[\text{La}(\text{LQQ})(\text{NO}_3)_3]$ , putative  $[\text{La}(\text{LQQ}^{\bullet-})(\text{NO}_3)_3]$  and  $[\text{La}(\text{LQQ}^{2-})(\text{NO}_3)_2]$  were optimized by density functional theory (DFT) methods and gave good agreement with XRD metrics (Table S5). All carbonyl IR stretches were well reproduced (Figures S38–40). In addition, a +0.51 V relative stabilization of  $[\text{La}(\text{LQQ}^{\bullet-})(\text{NO}_3)_3]$  cf.  $\text{LQQ}^{\bullet-}$  was predicted, compared to +0.61 V observed experimentally (Figure S37). Encouraged by the agreement of DFT calculations with experimental data, we examined possible mechanisms for the dehydrogenation of  $4^{\text{Me}}\text{BnOH}$  by  $[\text{La}(\text{LQQ})(\text{NO}_3)_3]$ .

The catalytic pathway of MDH has been considered to occur through one of two plausible mechanisms: hydride transfer (HT) or addition–elimination (AE).<sup>13</sup> Although the HT mechanism is generally accepted for biological MDH enzymes,<sup>14</sup> recent computational work on Ln-XoxF indicated a possible preference for the AE mechanism.<sup>15</sup>

In the current work, the HT mechanism was considered first (Figures 2a and S47–48). In the first calculated transition state (TS), a benzylic hydride was transferred to the C(2)-QQ carbon atom from  $4^{\text{Me}}\text{BnOH}$  with concerted alcohol deprotonation by a  $\text{NO}_3^-$  ligand (TS<sup>HT</sup>,  $\Delta G^\ddagger = 24.2 \text{ kcal mol}^{-1}$ ). This step afforded  $4^{\text{Me}}\text{PhCHO}$ ,  $\text{HNO}_3$  and the hemiacetal complex (Int2). Reprotonation of Int2 by  $\text{HNO}_3$  to the hemiacetal (Int<sup>HT</sup>) was nearly barrier-less. Enolization of Int<sup>HT</sup> was assisted by a  $\text{NO}_3^-$  ligand to give the catechol complex with an activation barrier of  $22.9 \text{ kcal mol}^{-1}$  (TS<sup>NO3</sup>). Explicit action of 2,6-lutidine reduced the barrier for enolization by ~15  $\text{kcal mol}^{-1}$  (TS<sup>Lut</sup>,  $\Delta G^\ddagger = 7.6 \text{ kcal mol}^{-1}$ ). Deprotonation of the catechol afforded dimeric  $[\text{La}(\text{LQQ}^{2-})(\text{NO}_3)_2]$ , which was downhill by ~35  $\text{kcal mol}^{-1}$ .

The AE mechanism was also examined (Figures 2b and S45–46). As expected,<sup>6b,c,14b,15</sup>  $\text{NO}_3^-$ -assisted addition of  $4^{\text{Me}}\text{BnOH}$  at the C(2)-QQ carbon atom to give the hemiketal complex (Int<sup>AE</sup>) had a low barrier of  $8.1 \text{ kcal mol}^{-1}$  (Figure 2b). The barrier for the subsequent retro-ene step (TS<sup>ene</sup>) to yield the catechol complex (Cat) and  $4^{\text{Me}}\text{PhCHO}$  was ~40  $\text{kcal mol}^{-1}$  and base did not facilitate this step. The activation energy for the retro-ene step was lowered (ateTS<sup>ene</sup>,  $\Delta G^\ddagger = 24.5 \text{ kcal mol}^{-1}$ ) from the deprotonated hemiketal complex (ateInt<sup>AE</sup>) as similarly calculated by others.<sup>15,16</sup> However, formation of ateInt<sup>AE</sup> over Int<sup>AE</sup> was only favored in the presence of DBU, but not weakly basic 2,6-lutidine (Figure 2b, dashed and dotted lines). Thus, in the presence of DBU,  $[\text{La}(\text{LQQ})(\text{NO}_3)_3]$  may oxidize  $4^{\text{Me}}\text{BnOH}$  by an AE mechanism, as reported for  $\text{Ca}^{2+}$ -PQQTME complexes.<sup>6b,c</sup>

Overall, our DFT study suggested that for the dehydrogenation of  $4^{\text{Me}}\text{BnOH}$  by  $[\text{La}(\text{LQQ})(\text{NO}_3)_3]$ : (i) in the absence of a base, the HT mechanism should be preferred with two free energy barriers of ~24  $\text{kcal mol}^{-1}$ , consistent with a slow reaction at r.t. (ii) under our catalytic conditions HT should



also be favored, as 2,6-lutidine should enhance the rate by facilitating the enolization process (iii) nitrate ligands are important in both mechanisms by acting analogously to the “proton-shuttle” pendant carboxylate in MDH enzymes.<sup>13–15</sup>

We have synthesized a functional model for the lanthanide-dependent XoxF-MDH enzyme. This complex dehydrogenated a benzyl alcohol stoichiometrically and catalytically under neutral and mildly basic conditions. DFT investigations suggested a HT mechanism for these reactions and, by extension, for MDH enzymes. Efforts to expand these studies are underway, for example, by gauging the impact of changing the nitrate coligands and/or the rare-earth cation on the catalytic activity of our model system.

## ■ ASSOCIATED CONTENT

### Supporting Information

The Supporting Information is available free of charge on the ACS Publications website at DOI: 10.1021/jacs.7b12318.

Synthetic procedures and spectroscopic data, NMR spectra from reaction mixtures, additional electrochemistry and computational data (PDF)

X-ray crystallography data (CIF)

## ■ AUTHOR INFORMATION

### Corresponding Author

\*schelter@sas.upenn.edu

### ORCID

Thibault Cheisson: 0000-0003-4359-5115

Eric J. Schelter: 0000-0002-8143-6206

### Notes

The authors declare no competing financial interest.

## ■ ACKNOWLEDGMENTS

We thank the U.S. NSF (CHE-1608925) and University of Pennsylvania for support of this work. The Camille and Henry Dreyfus Postdoctoral Program in Environmental Chemistry is acknowledged for a fellowship to T.C. This work used the Extreme Science and Engineering Discovery Environment, which is supported by the U.S. NSF, OCI-1053575.

## ■ REFERENCES

- (1) (a) Sirajuddin, S.; Rosenzweig, A. C. *Biochemistry* **2015**, *54*, 2283–2294. (b) Reid, M. F.; Fewson, C. A. *Crit. Rev. Microbiol.* **1994**, *20*, 13–56.
- (2) (a) Anthony, C. *Arch. Biochem. Biophys.* **2004**, *428*, 2–9. (b) Goodwin, P. M.; Anthony, C. *Adv. Microb. Physiol.* **1998**, *40*, 1–80.
- (3) (a) Hibi, Y.; Asai, K.; Arafuka, H.; Hamajima, M.; Iwama, T.; Kawai, K. *J. Biosci. Bioeng.* **2011**, *111*, 547–549. (b) Fitriyanto, N. A.; Fushimi, M.; Matsunaga, M.; Pertiwinigrum, A.; Iwama, T.; Kawai, K. *J. Biosci. Bioeng.* **2011**, *111*, 613–617. (c) Nakagawa, T.; Mitsui, R.; Tani, A.; Sasa, K.; Tashiro, S.; Iwama, T.; Hayakawa, T.; Kawai, K. *PLoS One* **2012**, *7*, e50480. (d) Pol, A.; Barends, T. R. M.; Dietl, A.; Khadem, A. F.; Eygensteyn, J.; Jetten, M. S. M.; Op den Camp, H. J. M. *Environ. Microbiol.* **2014**, *16*, 255–264.
- (4) Keltjens, J. T.; Pol, A.; Reimann, J.; Op Den Camp, H. J. M. *Appl. Microbiol. Biotechnol.* **2014**, *98*, 6163–6183.
- (5) (a) Friedle, S.; Reisner, E.; Lippard, S. J. *Chem. Soc. Rev.* **2010**, *39*, 2768–2779. (b) Koval, I. A.; Gamez, P.; Belle, C.; Selmecezi, K.; Reedijk, J. *Chem. Soc. Rev.* **2006**, *35*, 814. (c) Simmons, T. R.; Berggren, G.; Bacchi, M.; Fontecave, M.; Artero, V. *Coord. Chem. Rev.* **2014**, *270*–271, 127–150.
- (6) (a) Itoh, S.; Huang, X.; Kawakami, H.; Komatsu, M.; Ohshiro, Y.; Fukuzumi, S. *J. Chem. Soc., Chem. Commun.* **1995**, 2077–2078.

- (b) Itoh, S.; Kawakami, H.; Fukuzumi, S. *J. Am. Chem. Soc.* **1997**, *119*, 439–440. (c) Itoh, S.; Kawakami, H.; Fukuzumi, S. *Biochemistry* **1998**, *37*, 6562–6571. (d) Suzuki, S.; Sakurai, T.; Itoh, S.; Ohshiro, Y. *Inorg. Chem.* **1988**, *27*, 591–592. (e) Suzuki, S.; Sakurai, T.; Itoh, S.; Ohshiro, Y. *Nippon Kagaku Kaishi* **1988**, 421–424. (f) Tommasi, L.; Shechter-Barloy, L.; Varech, D.; Battioni, J.-P.; Donnadieu, B.; Verelst, M.; Bousseksou, A.; Mansuy, D.; Tuchagues, J.-P. *Inorg. Chem.* **1995**, *34*, 1514–1523. (g) Ernst, S.; Kasack, V. Z. *Naturforsch., B: Chem. Sci.* **1987**, *42b*, 425–430. (h) Kaim, W.; Kohlmann, S. *Inorg. Chem.* **1987**, *26*, 1469–1470. (i) Ernst, S.; Hänel, P.; Jordanov, J.; Kaim, W.; Kasack, V.; Roth, E. *J. Am. Chem. Soc.* **1989**, *111*, 1733–1738.
- (7) (a) Nakamura, N.; Kohzuma, T.; Kuma, H.; Suzuki, S. *Inorg. Chem.* **1994**, *33*, 1594–1599. (b) Wanner, M.; Sixt, T.; Klinkhammer, K.-W.; Kaim, W. *Inorg. Chem.* **1999**, *38*, 2753–2755. (c) Mitome, H.; Ishizuka, T.; Shiota, Y.; Yoshizawa, K.; Kojima, T. *Inorg. Chem.* **2013**, *52*, 2274–2276. (d) Mitome, H.; Ishizuka, T.; Shiota, Y.; Yoshizawa, K.; Kojima, T. *Dalton Trans.* **2015**, *44*, 3151–3158.
- (8) (a) Chen, Z. F.; Shi, Y. F.; Liu, Y. C.; Hong, X.; Geng, B.; Peng, Y.; Liang, H. *Inorg. Chem.* **2012**, *51*, 1998–2009. (b) Liu, Y.-C.; Chen, Z.-F.; Liu, L.-M.; Peng, Y.; Hong, X.; Yang, B.; Liu, H.-G.; Liang, H.; Orvig, C. *Dalton Trans.* **2009**, 10813–10823. (c) Wei, J.-H.; Chen, Z.-F.; Qin, J.-L.; Liu, Y.-C.; Li, Z.-Q.; Khan, T.-M.; Wang, M.; Jiang, Y.-H.; Shen, W.-Y.; Liang, H. *Dalton Trans.* **2015**, *44*, 11408–11419.
- (9) (a) Itoh, S.; Kawakami, H.; Fukuzumi, S. *J. Am. Chem. Soc.* **1998**, *120*, 7271–7277. (b) Dorfner, W. L.; Carroll, P. J.; Schelter, E. J. *Org. Lett.* **2015**, *17*, 1850–1853.
- (10) (a) Bogart, J. A.; Lewis, A. J.; Schelter, E. J. *Chem. - Eur. J.* **2015**, *21*, 1743–1748. (b) Robinson, J. R.; Booth, C. H.; Carroll, P. J.; Walsh, P. J.; Schelter, E. J. *Chem. - Eur. J.* **2013**, *19*, 5996–6004.
- (11) (a) Kawahara, R.; Fujita, K. I.; Yamaguchi, R. *J. Am. Chem. Soc.* **2012**, *134*, 3643–3646. (b) Gnanaprakasam, B.; Zhang, J.; Milstein, D. *Angew. Chem., Int. Ed.* **2010**, *49*, 1468–1471.
- (12) (a) Jia, Z.; Ramstad, T.; Zhong, M. *Electrophoresis* **2001**, *22*, 1112–1118. (b) Kaupmees, K.; Trummel, A.; Leito, I. *Croat. Chem. Acta* **2014**, *87*, 385–395.
- (13) (a) Anthony, C. *Biochem. J.* **1996**, *320*, 697–711. (b) Goodwin, M. G.; Anthony, C. *Biochem. J.* **1996**, *318*, 673–679. (c) Oubrie, A.; Dijkstra, B. W. *Protein Sci.* **2000**, *9*, 1265–1273. (d) Reddy, S. Y.; Bruice, T. C. *Protein Sci.* **2004**, *13*, 1965–1978. (e) Dewanti, A. R.; Duine, J. A. *Biochemistry* **2000**, *39*, 9384–9392.
- (14) (a) Kay, C. W. M.; Mennenga, B.; Görisch, H.; Bittl, R. *Proc. Natl. Acad. Sci. U. S. A.* **2006**, *103*, 5267–5272. (b) Idupulapati, N. B.; Mainardi, D. S. *J. Phys. Chem. A* **2010**, *114*, 1887–1896. (c) Zhang, X.; Reddy, S. Y.; Bruice, T. C. *Proc. Natl. Acad. Sci. U. S. A.* **2007**, *104*, 745–749. (d) Zheng, Y. J.; Xia, Z.-x.; Chen, Z.-w.; Mathews, F. S.; Bruice, T. C. *Proc. Natl. Acad. Sci. U. S. A.* **2001**, *98*, 432–434.
- (15) (a) Leopoldini, M.; Russo, N.; Toscano, M. *Chem. - Eur. J.* **2007**, *13*, 2109–2117. (b) Prejanò, M.; Marino, T.; Russo, N. *Chem. - Eur. J.* **2017**, *23*, 8652–8657.
- (16) Zheng, Y. J.; Bruice, T. C. *Proc. Natl. Acad. Sci. U. S. A.* **1997**, *94*, 11881–11886.